Global NEST Journal, Vol 23, No 1, pp 127-136

Impact of NaOH-surface treatment on emerging pollutant biosorption performance using marine algua, *Posidonia Oceanica*

Krika F.[1]*, Krika A.[2] and Azizi A.[3]
[1]University of Mohamed Seddik Ben Yahia, LIME Laboratory, Faculty of Sciences and Technology, BP 98 Ouled Aissa, 18000, Jijel, Algeria
[2]University of Mohamed Seddik Ben Yahia, Faculty of Nature Life and Sciences, Department of Environmental Sciences and Agronomic Sciences, BP 98 Ouled Aissa, 18000, Jijel, Algeria
[3]University of Amar Telidji, Faculty of Technology, BAS Laboratory, Highway Ghardaia Post Box G37 (M'kam) 03000, Laghouat, Algeria

Received: 04/03/2021, Accepted: 12/04/2021, Available online: 20/05/2021

*to whom all correspondence should be addressed: e-mail: f.krika@hotmail.fr

https://doi.org/10.30955/gnj.003579

Graphical abstract

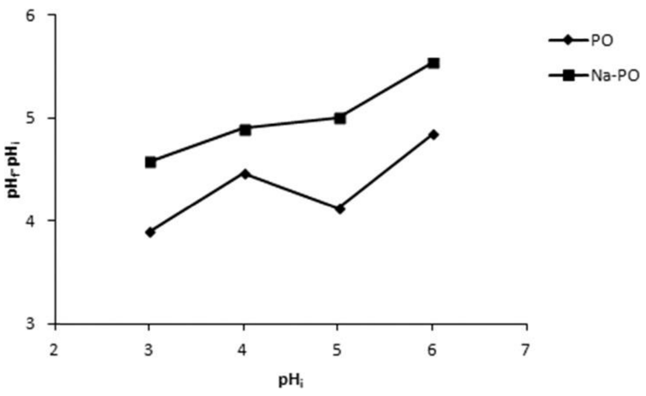

Abstract

In the present investigation, marine biomass (*Posidonia Oceanica*) (PO), in both its unmodified PO and basic-modified (Na-PO) forms, was studied for its possible utilisation as a cheap biosorbent for the retention of amoxicillin (AMX). Biosorption studies were carried out in a batch system and the effects of solution pH, biosorbent dose, initial AMX concentration, contact time and temperature were studied in detail. Characterization of the biosorbent was performed using Fourier transforms infra-red spectroscopy (FTIR) and pH_{PZC}. The biosorption of AMX was adjusted by Langmuir and Freundlich isotherm models, equilibrium isotherms were applicable with maximum monolayer biosorption capacity of 51.33 mg g^{-1} and 75.33 mg g^{-1} for PO and Na-PO, respectively. Kinetics investigations showed that both biosorbents followed the pseudo-second order. Thermodynamics studies indicated that the biosorption of AMX onto PO and Na-PO was spontaneous and endothermic in nature. These results proved that chemical modification of *Posidonia Oceanica* surface improved the biosorption properties of AMX.

Keywords: biosorption, AMX, Na-PO, thermodynamics

1. Introduction

Pharmaceuticals are substances that have biological activity and are used around the world to treat diseases in humans and animals. In recent years, consumption, use of the active substance (PhAC) and their release into the aquatic environment have given rise to growing concern. These compounds are part of emerging pollutants. Antibiotics are one of the main classes of PhAC. They enter aquatic environments via wastewater treatment plants (Gros *et al.*, 2010), via discharges from hospitals (Hartmann *et al.*, 1998), or even via groundwater (Sacher *et al.*, 2001). These uncontrolled releases cause adverse effects on these media.

Amoxicillin is one of the most widely used antibiotics worldwide. It is used to treat many infections. This compound has been recognized in recent years as an emerging pollutant because it causes toxic effects on the environment (Zouiten *et al.*, 2016). The intent of the magnitude of this problem has increased, by developing increasingly clean and efficient technologies to remove this compound from the aquatic environments.

Various remediation techniques were tested to remove amoxicillin from aqueous media including: ozonation (Andreozzi *et al.*, 2003), photo degradation (Trovó *et al.*, 2008), advanced oxidation processes (Ay et Kargi, 2010), la nano filtration (Moarefian *et al.*, 2014). However, these technologies have disadvantages and limitations; require high-tech operations, qualified personnel or expensive equipment. In addition, these methods can generate toxic waste and even incomplete removal. These disadvantages imply the need to develop new and effective methods for amoxicillin elimination (Kyzas *et al.*, 2015; Nanaki *et al.*, 2015).

Biosorption is considered as one of the mainly useful and efficient process to remove a variety of contaminants within wastewater (Moussavi *et al.*, 2015). This technique is easy and applicable at low cost using various adsorbent materials. The commercially available adsorbents are considered expensive, making their use infeasible in large scale operations. So, our effort has been focused to the use of a cheap biosorbent from marine biomass (*Posidonia*

Oceanica). Nevertheless, to the best of our knowledge, has not been found in the literature that *posidonia oceanica* has been used as biosorbent for AMX removal in both forms, i.e; its unmodified (PO) and basic-modified (Na-PO) forms.

Therefore, the main objective of our investigation is to study the enhancement of surface modification of the marine algae, Posidonia Oceanica, considered as an inexpensive and highly available lignocellulosic biomass, for the removal of AMX from aqueous media. The biomass was accurately characterized using Fourier transform infrared spectroscopy (FTIR) and pH_{PZC}. Besides, the experimental results were analyzed to study the kinetic, equilibrium and thermodynamic aspect of the biosorption to assess the biosorption performance of the developed biosorbent.

2. Materials and methods

2.1. Pollutant biosorption experiments

The biosorption studies were carried out in batch mode. A known amount of biosorbents was introduced in flasks containing certain concentration of AMX. The mixture was stirred during a determined time. While equilibrium was reached, the absorbance of supernatants was determined by spectrophotometer (Shimadzu UV-vis 1240) at the maximum absorbency visible wave length (λ_{max}= 227 nm).

The pH control on AMX biosorption against PO and Na-PO was studied at pH range of 3 to 9, via AMX initial concentration of 50 mg L^{-1} and shaking time of 180 min at 25 °C. The initial solution pH's was adjusted with dilute chlorhydric acid (0.1 M) and sodium hydroxide (0.1 M). The following kinetic, equilibrium and thermodynamic investigations were performed at optimal pH. Kinetic (two initial concentrations of AMX (50 and 100 mg L^{-1}), times varying from 1 to 240 min and equilibrium investigations (AMX concentrations ranging from 10 to 500 mg L^{-1} and shaking time of 90 min) were carried out at the interval of 25–45 °C. The data were used for the calculation of thermodynamic parameters.

The uptake of biosorbed pollutant per unit mass of biosorbents at equilibrium, q_e (mg g^{-1}), and the biosorption percentage, (% removal), were calculated using the following relationships:

$$q_e = \frac{(C_0 - C_e)}{m} \times V \qquad (1)$$

$$\%rate = \frac{(C_0 - C_e)}{C_0} \times 100 \qquad (2)$$

Where *V* is the volume of the solution (L), m is the mass of biosorbent (g), C_0 is the initial MB concentration (mg L^{-1}), Ce is the MB equilibrium concentration (mg L^{-1}) in liquid phase and q_e is the AMX quantity biosorbed at equilibrium (mg g^{-1}).

2.2. Kinetic and isotherm models

Biosorption rate is an important parameter that establishes the biosorption effectiveness of a biosorbent. It demonstrates the reaction pathways. The biosorption kinetics of AMX onto PO and Na-PO was tested using pseudo-first-order, pseudo-second-order and intra-particule diffusion models in order to understand the mechanism of control of the sorption system.

Biosorption isotherms are essential that elucidates the relationship between adsorbate and biosorbent and more reports the maximum adsorption amount. Therefore, Freundlich and Langmuir isotherm models were used to evaluate the biosorption equilibrium parameters of AMX onto PO and Na-PO. So as to evaluate the adjustment of the models to describe the biosorption of AMX onto PO and Na-PO, non-linear equations of kinetic and isotherm models (Table 1) were adjusted to experimental data using Excel software, as the nonlinear modelling is expected the better to estimate parameters of the used models, owning to the inherent bias, various estimation errors and fit distortions, what could be as a result from the linearization (Khan *et al.*, 2015).

To assess the consistency of all kinetic and isotherm models to explain AMX removal by PO and Na-PO, the coefficients of determination (R^2) and chi-square test analysis values (χ^2) were assessed. χ^2 was established using equation:

$$\chi^2 = \sum \frac{(q_{\exp,i} - q_{\mathrm{cal},i})^2}{q_{\mathrm{cal},i}} \qquad (3)$$

Where $q_{exp,i}$ and $q_{cal,i}$ are the equilibrium capacity (mg g^{-1}) obtained from the experiment and calculated from model, respectively.

Table 1. Non-linear equations of kinetic and isotherm models

	Kinetic models
Pseudo-first order	$q_t = q_e(1 - e^{-k_1 t})$
Pseudo-second order	$q_t = \frac{k_2 q_e^2 t}{1 + k_2 q_e t}$
Intraparticle diffusion	$q_t = k_{id} t^{0.5} + C$
	Isotherm models
Langmuir	$q_e = \frac{q_{max} K_L C_e}{1 + K_L C_e}$
Freundlich	$q_e = K_F C_e^{1/n}$

k_1 (min^{-1}) = rate constant of pseudo-first order; k_2 (g mg^{-1} min^{-1}) = rate constant of pseudo-second order; k_{id}(mg g^{-1} $min^{-0.5}$) = intraparticle diffusion rate constant; q_{max}(mg g^{-1}) = maximum adsorption capacity; K_L(L mg^{-1}) = Langmuir constant; K_f ((mg g^{-1}) (L mg^{-1})$^{1/n}$)= Freundlich constant; *n*= Freundlich exponent.

2.3. Thermodynamic analysis

The thermodynamic parameters that make it easy for us to identify the nature of the removal of AMX on raw and modified biosorbent are standard free energy change (ΔG°), standard enthalpy (ΔH°) and standard entropy (ΔS°) were determined using the following equations:

$$K_d = \frac{q_e}{C_e} \tag{4}$$

$$\Delta G^\circ = -RT \ln K_d \tag{5}$$

$$\ln K_d = \frac{\Delta S^\circ}{R} - \left(\frac{\Delta H^\circ}{R}\right)\frac{1}{T} \tag{6}$$

Where K_d: distribution constant; R: perfect gas constant (J mol $^{-1}$ K^{-1}); T: absolute temperature (K).

2.4. Chemicals

All reagents used ($C_{16}H_{19}N_3O_5S$, NaOH, H_2SO_4) were of analytical grade (Sigma-Aldrich). The Amoxicillin was kindly provided by SAIDAL® pharmaceutical company (Algeria). The AMX (Figure 1) stock solution was prepared by dissolving the appropriate quantity in distilled water.

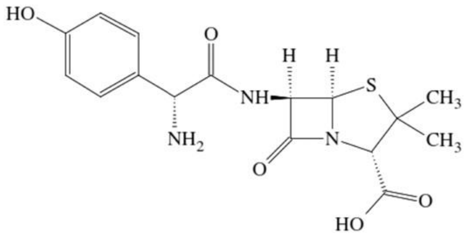

Figure 1. Chemical structure of amoxicillin

2.5. Raw and modified material

At first, Posidonia Oceanica (PO) was collected from Jijel coasts (Northeasthern Algeria) in September 2020, washed with distilled water, in order to eliminate impurities, and dried in oven at 50 ºC for 24 h. after that, the biomass was ground and granulometrically separated in particles with diameters between 0.3 and 0.5 mm. For the chemical modification, 20 g of biosorbent was impregnated with 200 mL of 1 M solution NaOH for 3 h. After that, biomass was filtered and washed with distilled water until neutral pH. The modified biosorbent, called Na-PO was then dried in an oven at 50°C for 24 h and stored for further use.

2.6. Chemical surface properties

The infrared spectra of PO, Na-PO, and Na-PO-AMX are illustrated in Figure 2 (A, B and C). The main characteristic bands of biosorbents are shown Table 2:

Table 2. Principal absorption bands of biosorbents

Wave numbers (cm^{-1})	Liaison Types
3500–4000	Overlapping O-H groups (carboxyl and phenols)and N-H stretching vibration
2925	Stretching vibrations of $-CH_2$
1625 and 1427	C=O axial deformation (aldehyde, lactone, ketone and carboxyl groups)
1073	C-O stretching of carboxylate and ether structures
500–600	Benzene derivatives

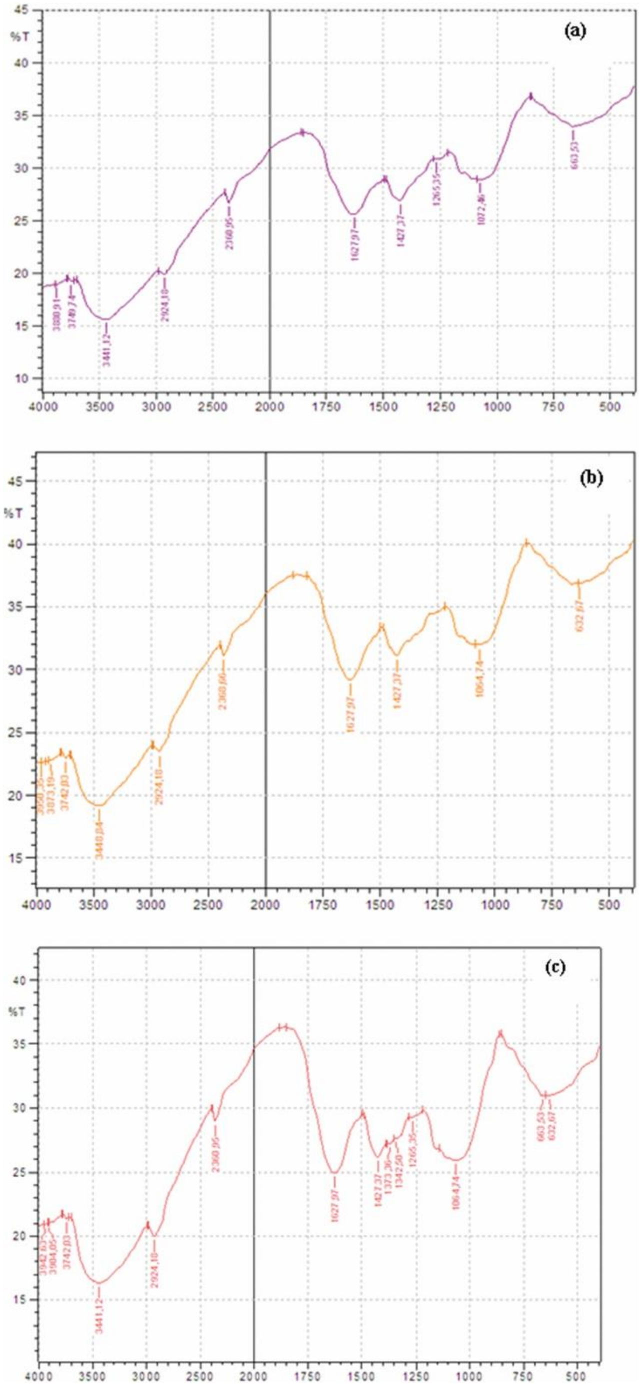

Figure 2. FTIR spectra for biosorbents: (a) PO, (b) Na-PO and (c) Na-PO-AMX

Positive or negative charges may appear on the surface of biosorbent depending on the pH of the medium. In general: if the pH> pH_{PZC}, pH_{PZC} (pH in which the number of negative charges is equal to that of positive charges so that the net charge of the solid is zero), there is a predominance of negative charges in the biosorbent, on the contrary if the pH <pH_{pzc} the particles of the solid are positively charged (Babic *et al.*,1999). The zero load point values obtained (Figure 3) (pH_{PZC} = 4.4 for PO and pH_{PZC} = 5.0 for Na-PO) reveal that both biosorbents are acidic in character.

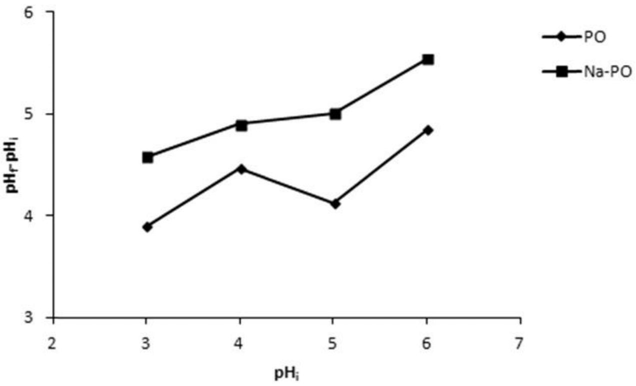

Figure 3. Determination of pHpzc of biosorbents

3. Results and discussion

3.1. Biosorption of AMX by raw and modified biosorbent

3.1.1. Effect of pH

The efficiency of the adsorption process strongly depends on the pH of the medium, since the variation of the pH could favour the modification of the charges of the adsorbent materials and of the adsorbate molecules (Samarghandi *et al.*, 2015).

AMX can exist in different forms in aqueous media due to the ionization of its three functional groups. At pH <pKa_1, AMX is protonated as follows $COOH/NH_3^+/OH$ (AMX^+). At pH values between pKa_1 and pKa_2 the carboxylic group will be deprotonated COO^-/NH_3^+ /OH ($AMX^\pm$), while at pH values between pKa_2 and pKa_3 the carboxylic and amine groups will be deprotonated $COO^-/NH_2/OH$ (AMX^-). Finally, at pH> pKa_3, the phenolic hydroxyl will also be deprotonated $COO^-/NH_2/OH^-$, (AMX^{2-}) (Moussavi *et al.*, 2013).

Figures 4 and 5 show the distribution of AMX species as a function of pH, as well as the effect of pH on the adsorption of AMX by PO and Na-PO in the range of pH 3 to 9, in which there is a predominance of the species $AMX^\pm$ and AMX^-. Figure 5 shows that both biosorbents exhibit good adsorption capacity towards AMX at all pH ranges studied (> 40 mg g^{-1} for PO and > 50 mg g^{-1} for Na-PO), which indicates that several mechanisms may be involved in addition to the electrostatic interaction, such as the formation of hydrogen bonds, electron donor-acceptor and the π- π dispersion interaction π (Martins *et al.*, 2016).

The low adsorption capacity for both biosorbents was recorded at pH 9 (43 mg g^{-1} for PO and 57.2 mg g^{-1} for Na-PO). This can be explained by the fact that AMX and the surface of both biosorbents are negatively charged (pH_{PZC} = 4.4 for PO and pH_{PZC} = 5.0 for Na-PO) which results in electrostatic repulsion. On the other hand, at pH values lower than pH_{PZC}, the surface of the two biosorbents is positively charged, increasing their adsorption capacities for AMX, which is in the zwitterion form (pH = 3.0–6.0) (Adriano *et al.*, 2005).

Similar results were reported by Moussavi *et al.*, 2013. Furthermore, we find that the modification of the surface has no influence on the optimum pH. Indeed, at pH 4.0 the adsorption capacity increases from 86.95 mg g^{-1} for PO to 115.62 mg g^{-1} for Na-PO resulting in 24.80% increase in adsorption capacity. This can be explained by the fact that the NaOH treatment removes lignin which colors the biosorbent and which can interfere with the retention of pollutants. This type of treatment develops pores in the biosorbent and therefore provides a larger surface area and pore volume for the biosorbent (Yan *et al.*, 2015).

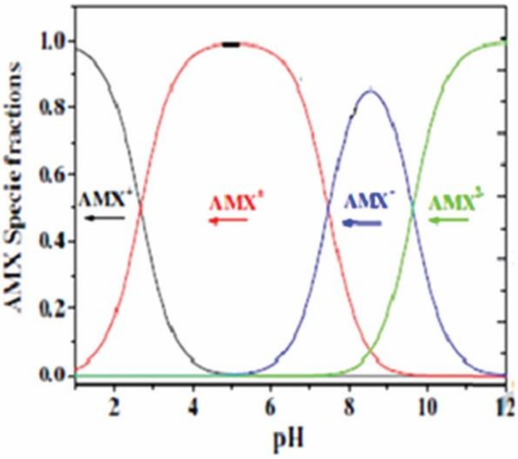

Figure 4. Distribution of AMX species as function of pH (Pezoti *et al.*, 2015)

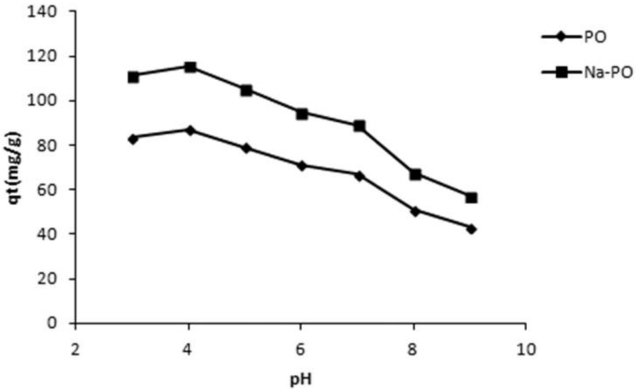

Figure 5. Effect of pH on AMX removal

3.1.2. Effect of biosorbent dose

The effect of the dose of biosorbent on the elimination of AMX was studied by varying the mass of the two biosorbents (Figure 6).

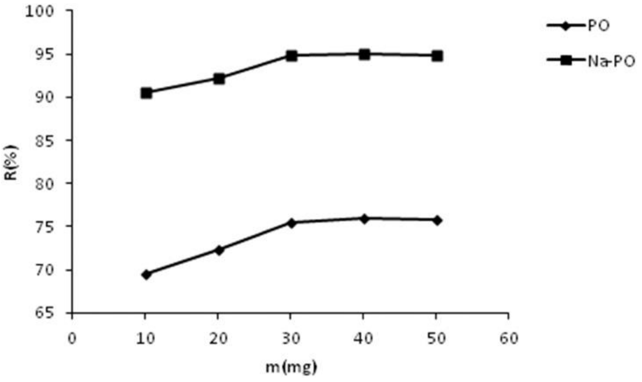

Figure 6. Effect of biosorbents dose on AMX removal

The percentage retention of AMX increases from 69.55% to 75.76% and from 90.5% to 94.87% by increasing the mass of PO and Na-PO from 400 mg L^{-1} to 2000 mg L^{-1}. The increase in the retention percentage of AMX as a function of the increase in the mass of biosorbents is mainly due to a consequent increase in the surface area and consequently the number of active adsorption sites (Chen *et al.*, 2010). In addition, Figure 6 also shows that by further increasing the dose of biosorbent beyond 1200 mg L^{-1}, the removal of AMX by PO remains constant, possibly due to saturation of the active sites of adsorption. Likewise, for Na-PO. The results also showed that Na-PO is a more efficient biosorbent (R = 94.89%) for AMX removal than PO (R = 75.49%).

3.1.3. Adsorption kinetics

Figure 7 (A and B) exhibit the kinetic of AMX elimination on PO and Na-PO for the entire concentration range studied. The experimental results show that the contact time of 35min is adequate to reach equilibrium and the biosorption stay constant with further raise in contact time. To assess the better kinetic model to report the biosorption of AMX by PO and Na-PO, pseudo-first order and pseudo-second kinetic models were adjusted to experimental data and their non-linear fitting are exposed in Figure 8(A and B) and 9 (A and B), respectively. Table 3 (A and B**)** records studied kinetic models parameters. Depending on the quantity sorbed at equilibrium qe, high values of determination coefficient R^2 (0.994–0.997) and lowest values of chi-square test analysis χ^2 (0.12-0.38), pseudo-second order model is suitable to describe the kinetic data for both biosorbents, signifying that the AMX biosorption onto PO and Na-PO mainly occurs by chemisorptions (Ho, 2006). Similar results were found by Martins *et al.*, 2015, using NaOH activated carbon for biosorption of tetracycline and by Huang *et al.*, 2012, using cyclodextrin-based biosorbent for biosorption of copper.

Table 3 (A). Kinetic parameters of pseudo-first order and pseudo-second order models for AMX biosorption on PO

C_0 (mg L^{-1})	Pseudo-first order					Pseudo-second order			
	$q_{e,exp}$ (mg g^{-1})	$q_{e,cal}$ (mg g^{-1})	k_1 (min^{-1})	R^2	χ^2	q_{cal} (mg g^{-1})	k_2 (mg g^{-1}.min^{-1})	R^2	χ^2
50	31.68	10.19	0.049	0.530	89.75	32.45	0.009	0.9994	0.12
100	53.85	15.82	0.021	0.387	166	52.03	0.008	0.9979	0.38

Table 3 (B). Kinetic parameters of pseudo-first order and pseudo-second order models for AMX biosorption on Na-PO

C_0 (mg L^{-1})	Pseudo-first order					Pseudo-second order			
	$q_{e,exp}$ (mg g^{-1})	$q_{e,cal}$ (mg g^{-1})	k_1 (min^{-1})	R^2	χ^2	q_{cal} (mg g^{-1})	k_2 (mg g^{-1}.min^{-1})	R^2	χ^2
50	39.3	15.90	0.056	0.60	101.7	40.29	0.007	0.9995	0.16
100	74.97	20.43	0.039	0.2835	428.6	76.62	0.003	0.9994	0.33

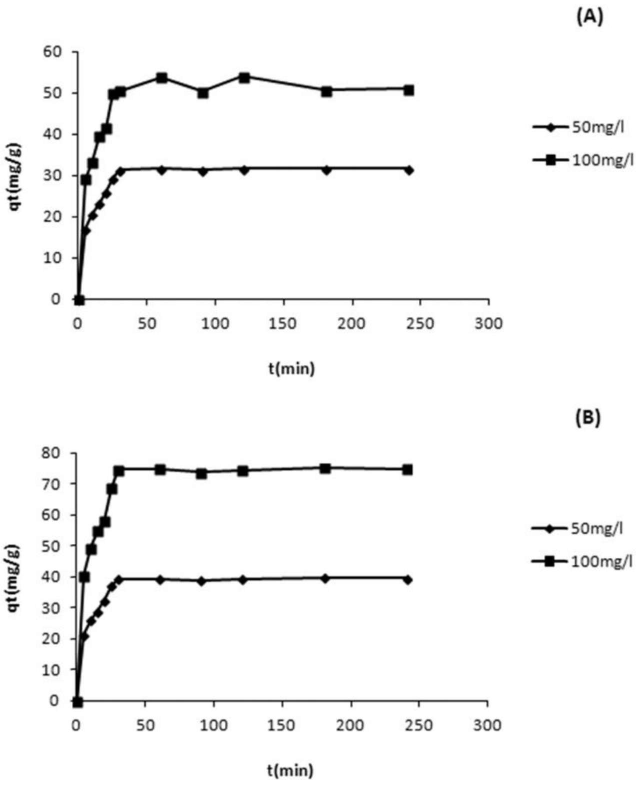

Figure 7. Kinetic elimination of AMX: (A):PO, (B): Na-PO.

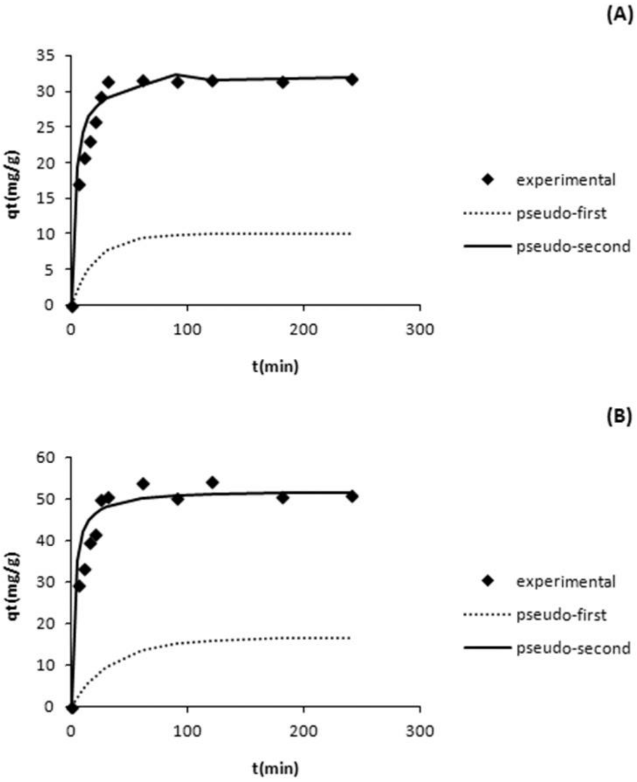

Figure 8. Non-linear adjustments of pseudo-first order and pseudo-second order kinetic models for biosorption of AMX on PO (A):50 mg L^{-1}, (B): 100 mg L^{-1}.

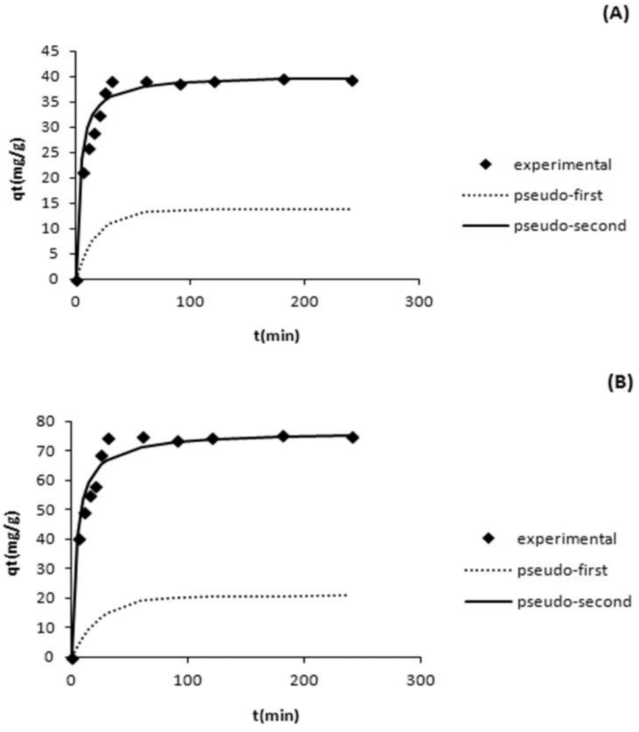

Figure 9. Non-linear adjustments of pseudo-first order and pseudo-second order kinetic models for biosorption of AMX on Na-PO (A):50 mg L^{-1}, (B): 100 mg L^{-1}

Moreover, diffusion model has been used to explain the mechanism of diffusion and the biosorption-controlling step. Usually, the intraparticle diffusion model (Weber and Morris, 1963) is related to surface and pore diffusion. This model is represented as:

$$q_t = k_{id} t^{0.5} + C \tag{7}$$

where k_{id} (mg g min$^{-0.5}$)) is the intraparticle rate constant and C is a constant associated to the thickness of the boundary layer. k_{id} and C values are listed in Table 4 (A and B) It is clear from Figure 10 (A and B) that principally three stages are implicated in AMX biosorption onto PO and Na-PO. The first part represents instant biosorption on the external surface. The progressive coverage of active sites owing to intraparticle diffusion of AMX onto PO and Na-PO is exhibited by the next step. The rate diminution in the intraparticle diffusion as a consequence to weak adsorbate concentration and lesser accessibility of active sites is reported by the last stage (Zhao *et al.*, 2018). Considering Equation 7, if the plot of q_t vs $t^{0.5}$ is a straight line and passes via the origin, the phenomenon of intraparticle diffusion controls the kinetics of biosorption. Though, the plots show many linearity and diverge from the origin (Figure 10 A and B), who involves that intraparticle diffusion is not the only rate-determining stage. Furthermore, lower values of C constant for both biosorbents (6.79-12.36 for PO and 8.14-16.41 for Na-PO) expose a small boundary layer effect.

Table 4 (A). Intraparticle diffusion model parameters for AMX biosorption onto PO.

C_0 (mg L^{-1})	K_{id} (mg L^{-1} min$^{-0.5}$)	C	R^2
50	4.44	6.79	0.986
100	7.01	12.36	0.951

Table 4 (B). Intraparticle diffusion model parameters for AMX biosorption onto Na-PO

C_0 (mg L^{-1})	K_{int} (mg L^{-1} min$^{-0.5}$)	C	R^2
50	5.63	8.14	0.984
100	10.25	16.41	0.962

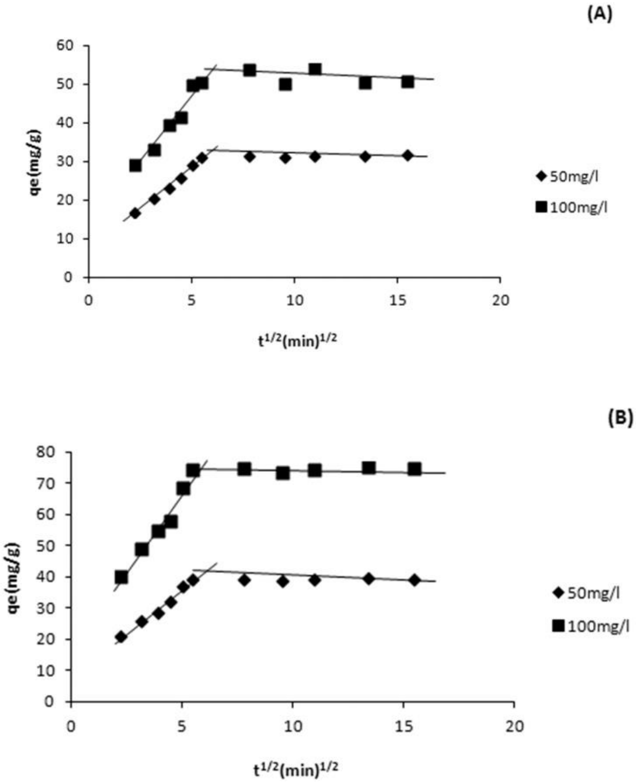

Figure 10. Intraparticle diffusion plots for biosorption of AMX onto: (A)=PO and (B)=Na-PO

3.1.4. *Biosorption isotherms*

Biosorption isotherm is an essential step that elucidates the interference between ad-sorbate and surface of biosorbent and more illustrates the maximum biosorption capaci-ty. To describe the AMX removal by PO and Na-PO, and to find the better-adjustment model, the non-linear form of Langmuir and Freundlich isotherm models were fitted to experimental results at 298, 308 and 318 K (Figure 11 and 12).

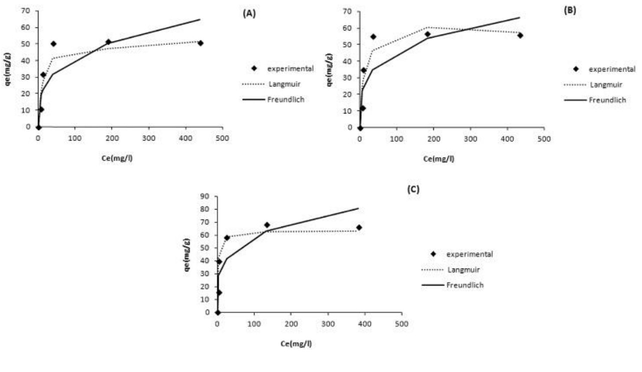

Figure 11. Non-linear adjustments of Langmuir and Freundlich isotherm models for biosorption of AMX onto PO (A) 298 K, (B) 308 K and (C) 318 K

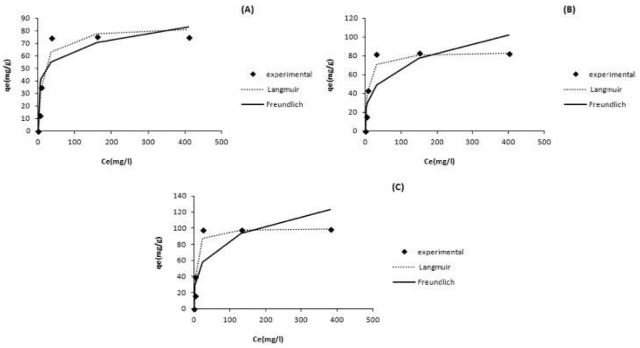

Figure 12. Non-linear adjustments of Langmuir and Freundlich isotherm models for biosorption of AMX onto Na-PO (A) 298 K, (B) 308 K and (C) 318 K

Freundlich's model (Freundlich, 1906) expresses a multi-layer biosorption with interference among biosorbed molecules on heterogeneous surfaces, admitting that biosorbent interface sites have a spectrum of diverse binding energies (Yang *et al.*, 2015).

Langmuir's model (Langmuir, 1918) assumes that the surface of the biosorbent is homogeneous in terms of energy. It also presumes that active sites are limited and no interference is present among the biosorbed molecules. It supposes that the maximum removal take place with the formation of mono-layer on the biosorbent interface and there is no changing of adsorbate molecules in the interface plane. The parameters of the Langmuir and Freundlich models are listed in Table 5 (A and B). As shown in this table, Langmuir isotherm model better fit the experimental data compared to Freundlich model. This is confirmed by the high values of correlation coefficients R^2 (0.9965-0.9997 for PO and 0.9962-0.9993 for Na-PO) and the low values chi-square test analysis χ^2 (0.004-0.18 for PO and 0.09-2.48 for Na-PO). Parameter 1/n indicates the favourability of biosorption as $1/n < 1$. The examination of the results reveals that the AMX removal onto PO and Na-PO is mono-layer coverage of the adsorbate on a biosorbent interface at regular temperature. We find that as the temperature increases, the maximum sorption capacity, q_m, increases significantly, from 52.63 mg g^{-1} to 63.37 mg g^{-1} and from 83.33 mg g^{-1} to 100 mg g^{-1} for PO and Na-PO, respectively, when the temperature rises from 298 K to 318 K. In addition, the value of Langmuir's constant, b, also increases with temperature for both biosorbents. These results suggest that an increase in temperature enhances removal of AMX by PO and Na-PO, which confirms the endothermic nature of biosorption of AMX onto both biosorbents.

Table 5(A). Isothermal parameters of Langmuir and Freundlich models for AMX biosorption onto PO

T (K)	Langmuir				Freundlich			
	q_m (mg g^{-1})	K_L (L mg^{-1})	R^2	χ^2	K_F ((mg g^{-1})·(L mg^{-1})$^{1/n}$)	$1/n$	R^2	χ^2
298	52.63	0.089	0.9965	0.18	10.55	0.30	0.4842	21.54
308	57.47	0.12	0.9971	0.13	13.80	0.26	0.4319	24.23
318	63.37	0.48	0.9997	0.004	21.18	0.21	0.5743	19.65

Table 5(B). Isothermal parameters of Langmuir and Freundlich models for AMX biosorption onto Na-PO

T (K)	Langmuir				Freundlich			
	q_m (mg g^{-1})	K_L (L mg^{-1})	R^2	χ^2	K_F ((mg g^{-1})·(L mg^{-1})$^{1/n}$)	$1/n$	R^2	χ^2
298	83.33	0.087	0.9962	2.48	29.83	0.17	0.5731	27.36
308	84.10	0.17	0.9987	0.09	18.19	0.29	0.5838	36.53
318	100	0.25	0.9993	0.10	23.52	0.28	0.6108	43.75

In addition, Table 5 (A and B) also illustrates the effect of surface modification on the biosorption capacity. At the same temperature, we see a significant increase in the retention of AMX (at 298 K, q_m increases from 51.43 mg g^{-1} for PO to 75.33 mg g^{-1} for Na-PO resulting from an increase of 46.60% in biosorption capacity) indicating a favourable effect of using NaOH treatment on improving biosorption capacity.

The essential characteristic of the Langmuir isotherm can be expressed by a dimensionless constant called the separation factor or equilibrium parameter, R_L, defined by the following expression:

$$R_L = \frac{1}{1 + bC_i} \tag{8}$$

Or: b: Langmuir constant, C_i: Initial AMX concentration.

The constant R_L indicates the type of isotherm, so that for values between 0 and 1 sorption is favorable (Aravindhan *et al.*, 2004). In Figure 13 (A and B) the R_L values are shown as a function of the initial AMX concentration in the temperature range studied. Note that, for both biosorbents, the R_L values are between 0 and 1 for all the experimental conditions employed indicating that the retention of AMX by PO and Na-PO is a favourable process.

The values of the maximum biosorption capacity found for PO and Na-PO are compared to those obtained by other researchers in Table 6. It shows that the maximum biosorption capacity for both biosorbents is greater than that found in the literature, indicating the great potential elimination of PO and Na-PO towards AMX.

3.2. Thermodynamic investigation

The calculated thermodynamic parameters are summarized in Table 7 (A and B). The values of ΔH° and ΔS° were determined from the slope and the intercept of the Van't Hoff equation (Equation 6).

Table 7 (A and B) shows that the free energy (ΔG°) values are negative at all studied temperatures, which confirms the spontaneous and the feasibility biosorption of AMX for both biosorbents. We also notice that ΔG decreases with increasing in temperatures suggesting AMX biosorption onto PO and Na-PO is favorable at higher temperature (Fu *et al.*, 2015). Furthermore, the positive values of ΔH, indicate the endothermic nature of bio-sorption on the surface of biosorbents, once the physisorption is still exothermic (Rathod *et al.*, 2015). The positive values of ΔS for PO and Na -PO suggests increased disorder at the solid/liquid interface during the biosorption process.

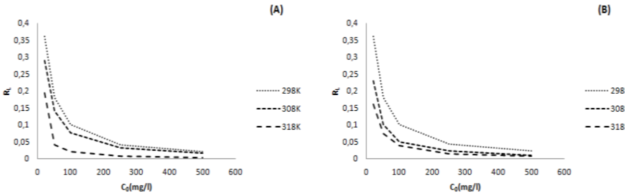

Figure 13. Separation constant (R_L) for biosorption of AMX onto (A): PO and (B): Na-PO

Table 6. Comparison of maximum adsorption capacity (q_m) of AMX for various biosorbents

Biosorbent	q_m(mg g^{-1})	References
PO	51,43	Present study
Na-PO	75.33	Present study
MWAC	75,8	Chayid et Ahmed, 2015
Chitosan grain	8.71	Adriano *et al.*, 2005
ASCK	282.42	Benjedim *et al.*, 2020
ASK	228.39	Benjedim *et al.*, 2020
CACOS	57	Limousy *et al.*, 2016
AC	221.9	Putra *et al.*, 2009
ACNPVW	2.69	Pouretedal et Sadegh, 2014
ACAF	265.2	Balarak *et al.*, 2017

AC: Activated carbon; MWAC: Magnetic waste tyre activated carbon; ASCK: NaOH modified Argan waste carbon; ASK: NaOH modified Argan waste; CACOS: A chemical-activated carbon of olive stones; AC-NPVW: Activated carbon nanoparticles prepared from vine wood; ACAF: Activated carbon prepared from Azolla filiculoides.

Table 7(A). Thermodynamic parameters for biosorption of AMX onto PO

T **(K)**	**Δ*H*° (Kcal mol^{-1})**	**Δ*S*° (Kcal mol^{-1})**	**Δ*G*° (Kcal mol^{-1})**	***R*²**
298	12.72	0.045	-0.76	0.853
308			-1.02	
318			-1.66	

Table 7(B). Thermodynamic parameters for biosorption of AMX onto Na-PO

T **(K)**	**Δ*H*° (Kcal mol^{-1})**	**Δ*S*° (Kcal mol^{-1})**	**Δ*G*° (Kcal mol^{-1})**	***R*²**
298	6.08	0.022	-0.44	0.948
308			-0.61	
318			-0.88	

4. Conclusion

The objective of the present investigation was to study the impact of chemical modification of the surface on the biosorption capacity of a marine plant, *Posidonia oceanica*, in order to obtain a high-performance biosorbent used to eliminate an emerging pollutant, amoxicillin, which may be present in the effluents of the pharmaceutical industry.

We have drawn conclusions about the importance of the chemical modification of the surface and the adsorption of this pollutant as a function of the pH of the media, the mass of the adsorbent, the absorption kinetics and the temperature:

- The adsorption equilibrium is reached after 30 minutes of contact for the PO and Na-PO;
- The influence of pH on the elimination of AMX shows that the quantity of pollutant adsorbed is greater the more the pH is acidic for PO. The same tendency was observed for Na-PO;
- The results observed for the mass of the two adsorbents show that there is an improvement in the yields when the mass of the adsorbent increases up to a certain dose beyond that, the removal of AMX is practically constant;
- The experimental kinetic and equilibrium models were better fitted by the pseudo-order 2 and Langmuir models, respectively, suggesting that the adsorption of AMX by PO and Na-PO is mainly carried out by chemisorption, resulting in a maximum monolayer adsorption capacity of 75.33 mg g^{-1} for Na-PO, greater than that obtained for PO (51.33 mg g^{-1}), greater than several adsorbents found in literature;
- The thermodynamic parameters revealed the spontaneity of the adsorption of AMX (ΔG° = -0.76 Kcal mol^{-1} for PO and ΔG° = -0.44 Kcal mol^{-1} for Na-PO at 298 K) and its endothermic characteristic (ΔH° = 12.72 Kcal mol^{-1} for PO and ΔH°= 6.0 Kcal mol^{-1} for Na-PO at 298 K);

At the end of this investigation, we can conclude that the chemical modification of the surface of the adsorbent by NaOH significantly increased its adsorption capacity. Therefore, Na-PO is considered to be an adsorbent with significant efficiency for AMX removal.

References

Adriano W.S., Veredas V., Santana C.C. and Golçalvez L.R.B. (2005), Adsorption of amoxicillin on chitosan beads: kinetics, equilibrium and validation of finite batch models, *Biochemical Engineering Journal,* **27**, 132–137.

Adriano W.S., Veredas V., Santana C.C. and Golçalvez L.R.B. (2005), Adsorption of amoxicillin on chitosan beads: kinetics, equilibrium and validation of finite batch models, *Biochemical Engineering Journal*, **27**, 132–137.

Andreozzi R., Caprio V., Marotta R. and Radovnikovic A. (2003), Ozonation and H_2O_2/UV treatment of clofibric acid in water: a kinetic investigation, *Journal of Hazardous Materials,* **103**(3), 233–246

Aravindhan R., Madhan B., Rao J.R. and Nair B.U. (2004), Recovery and reuse of chromium from tannery wastewaters using Turbinaria ornata seaweed, *Journal of Chemical Technology and Biotechnology*, **79**, 1251–1258.

Ay F. and Kargi F. (2010), Advanced oxidation of amoxicillin by Fenton's reagent treatment, *Journal of Hazardous Materials*, **179**(1–3), 622–627.

Babic B.M., Milonjic S.K., Polovina M.J. and Kaludierovic B.V. (1999), Point of zero charge and intrinsic equilibrium constants of activated carbon cloth, *Carbon*, **37**, 477–481.

Balarak D., Mostafapour F.K., Akbari H. and Joghtaei A. (2017), Adsorption of Amoxicillin Antibiotic from Pharmaceutical Wastewater by Activated Carbon Prepared from Azolla filiculoides, *Journal of Pharmaceutical Research International*, **8**(3), 1–13.

Benjedim S., Romero-Cano L.A., Pérez-Cadenas A.F., Bautista-Toledo M.I., Lotfi E. and Carrasco-Marín F. (2020), Removal of emerging pollutants present in water using an E-coli biofilm supported onto activated carbons prepared from argan wastes: Adsorption studies in batch and fixed bed, *Science of the Total Environment*, **720**, 137491.

Chayid M.A. and Ahmed M.J. (2015), Amoxicillin adsorption on microwave prepared activated carbon from Arundo donax Linn: Isotherms, kinetics, and thermodynamics studies, *Journal of Environmental Chemical Engineering,* **3**, 1592–1601.

Chen S., Zhang J., Zhang C., Yue Q., Li Y. and Li C. (2010), Equilibrium and kinetic studies of methyl orange and methyl violet adsorption on activated carbon derived from Phragmites australis, *Desalination*, **252,** 149–156

Freundlich H. (1906), Adsorption in solution, *Physical Chemistry Society*, **40**, 1361–1368.

Fu J., Chen Z., Wang M., Liu S., Zhang J., Zhang J., Han R. and Xu Q. (2015), Adsorption of methylene blue by a high-efficiency adsorbent (polydopamine microspheres): Kinetics, isotherm, thermodynamics and mechanism analysis, *Chemical Engineering Journal*, **259**, 53–61.

Gros M., Petrović M., Ginebreda A. and Barceló D. (2010), Removal of pharmaceuticals during wastewater treatment and environmental risk assessment using hazard indexes, *Environment International*, **36**, 15–26.

Hartmann A., Alder A.C., Koller T. and Widmer R.M. (1998), Identification of fluoroquinolone antibiotics as the main source of umuC genotoxivity in native hospital wastewater, *Environmental Toxicology and Chemistry*, **17**, 377–382.

Ho Y.S. (2006), Review of second-order models for adsorption systems, *Journal of Hazardous Materials B*, **136,**681–689.

Huang Z., Liu S., Zhang B., Xu L. and Hu X. (2012), Equilibrium and kinetics studies on the absorption of Cu(II) from the aqueous phase using a -cyclodextrin-based adsorbent, *Carbohydrate Polymers*, **88**, 609–617.

Khan T.A., Khan E.A. and Shahjahan (2015), Removal of basic dyes from aqueous solution by adsorption onto binary iron-manganese oxide coated kaolinite: Non-linear isotherm and kinetics modeling, *Applied Clay Science,* **107**, 70–77.

Kyzas G.Z., Fuc J., Lazaridis N.K., Bikiaris D.N. and Matis K.A. (2015), New approaches on the removal of pharmaceuticals from wastewaters with adsorbent materials, *Journal of Molecular Liquids*, **209**, 87–93.

Langmuir I. (1918), The adsorption of gases on plane surfaces of glass, mica and platinum, *Journal of American Chemistry Society*, **40**, 1361–1368.

Limousy L., Ghouma I., Ouederni A.M. and Jeguirim M. (2017), Amoxicillin removal from aqueous solution using activated carbon prepared by chemical activation of olive stone, *Environmental Science and Pollution Research Volume*, **24**, 9993–10004.

Martins A.C., Pezoti O., Cazetta A.L., Bedin K.C., Yamazaki D.A.S., Bandoch G.F.G., Asefa T., Visentainer J.V. and Almeida V.C. (2015), Removal of tetracycline by NaOH-activated carbon produced from macadamia nut shells: Kinetic and equilibrium studies, *Chemical Engineering Journal*, **260**, 291–299.

Moarefian A., Golestani H.A. and Bahmanpour H. (2014), Removal of amoxicillin from wastewater by self-made Polyethersulfone membrane using nanofiltration, *Journal of Environmental Health Science & Engineering,* **12**(1),1–10.

Moussavi G., Alahabadi A., Yagheian K. and Eskandari M. (2013), Preparation, characterization and adsorption potential of the NH_4Cl-induced activated carbon for the removal of amoxicillin antibiotic, *Chemical Engineering Journal,* **217**, 199–128.

Moussavi G., Alahabadi A., Yagheian K. and Eskandari M. (2013), Preparation, characterization and adsorption potential of the NH_4Cl-induced activated carbon for the removal of amoxicillin antibiotic, *Chemical Engineering Journal*, **217**, 199–128.

Moussavi G., Alahabadi A., Yaghmaeian K. and Eskandari M. (2013), Preparation, characterization and adsorption potential of the NH_4Cl-induced activated carbon for the removal of amoxicillin antibiotic from water, *Chemical Engineering Journal*, **217**,119–128.

Nanaki S.G., Kyzas G.Z., Tzereme A., Papageorgiou M., Kostoglou M., Bikiaris D.N. and Lambropoulouc D.A. (2015), Synthesis and characterization of modified carrageen an micro particles for the removal of pharmaceuticals from aqueous solutions, *Colloids and Surfaces B: Biointerfaces*, **127**, 256–265.

Pezoti O., Cazetta A.L., Bedin K.C., Souza L.S., Martins A.C., Silva T.L., Santos Júnior O.O., Visentainer J.V. and Almeida V.C. (2015), NaOH-activated carbon of high surface area produced from guava seeds as a high-efficiency adsorbent for amoxicillin removal: Kinetic, isotherm and thermodynamic studies, *Chemical Engineering Journal*, **288**, 778–788.

Pouretedal H.R. and Sadegh N. (2014), Effective removal of Amoxicillin, Cephalexin, Tetracycline and Penicillin G from aqueous solutions using activated carbon nanoparticles prepared from vine wood, *Journal of Water Process Engineering,* **1**, 64–73.

Putra E.K., Pranowo R., Sunarso J., Indraswati N. and Ismadji S. (2009), Performance of activated carbon and bentonite for adsorption of amoxicillin from wastewater: Mechanisms, isotherms and kinetics, *Water Research,* **43**, 2419–2430.

Rathod M., Haldar S. and Basha S. (2015), Nanocrystalline cellulose for removal of tetracycline hydrochloride from water via biosorption: Equilibrium, kinetic and thermodynamic studies, *Ecological Engineering*, **84**, 240.

Sacher F., Langea F.T., Braucha H. and Blankenhorn I. (2001), Pharmaceuticals in groundwaters. Analytical methods and results of a monitoring program in Baden-Württemberg, *Germany*. *Journal of Chromatography A*, **938**, 199–210.

Samarghandi M.R., Al-Musawi T.J., Mohseni-Bandpi A. and Zarrabi M. (2015), Adsorption of cephalexin from aqueous solution using natural zeolite and zeolite coated with manganese oxide nanoparticles, *ournal of Molecular Liquids,* **211**, 431–441.

Trovó A.G., Melo S.A.S. and Nogueira R.F.P. (2008), Photodegradation of the pharmaceuticals amoxicillin, bezafibrate and paracetamol by the photo-Fenton process—application to sewage treatment plant effluent, *Journal of Photochemistry and Photobiology A: Chemistry*, **198**(2–3), 215–220.

Weber W.J. and Morris J.C. (1963), Kinetics of adsorption on carbon from solution, *Journal of the Sanitary Engineering Division*, **2**, 31−60.

Yan Z., Li J., Chang S., Cui T., Jiang Y., Yu M., Zhang L., Zhao G., Qi P. and Li S. (2015), Lignin relocation contributed to the alkaline pretreatment efficiency of sweet sorghum bagasse, *Fuel*, **158**, 152–158.

Yang J., Yu M. and Chen W. (2015), Adsorption of hexavalent chromium from aqueous solution by activated carbon prepared from longan seed: Kinetics, equilibrium and thermodynamics, *Journal of Industrial and Engineering Chemistry,* **21**, 414–422.

Zhao Y., Li W., Liu Z., Liu J., Zhu L., Liu X. and Huang K. (2018), Renewable Tb/Eu-Loaded Garlic Peels for Enhanced Adsorption of Enrofloxacin: Kinetics, Isotherms, Thermodynamics, and Mechanism. *ACS Sustainable Chemistry & Engineering,* **6**, 15264−15272.

Zouiten A., Beltifa A., Van Loco J., Ben Mansour H. and Reyns T. (2016), Ecotoxicological potential of antibiotic pollution–industrial wastewater: bioavailability, biomarkers, and occurrence in Mytilus galloprovincialis, *Environmental Science and Pollution Research*, **23**(15), 15343–15350.